# Early Stages of Crystallization of Sol−Gel-Derived Lead Zirconate Titanate Thin Films

A. Wu,[†] P. M. Vilarinho,*[,†] I. Reaney,[‡] and I. M. Miranda Salvado[†]

*Ceramics and Glass Engineering Department, CICECO, University of Aveiro, 3810-193 Aveiro, Portugal, and Department of Engineering Materials, University of Sheffield, Sheffield S1 3JD, United Kingdom*

*Received August 8, 2002. Revised Manuscript Received December 13, 2002*

This article reports on the early stages of nucleation and growth and texture development of the perovskite phase in PZT(52/48) seeded and unseeded sol−gel thin films. Transmission electron microscopy (TEM) and X-ray diffraction (XRD) revealed that, in seeded films, the perovskite phase nucleates and grows at the film surface, on seed particles and at the Pt/PZT interface. In contrast, for unseeded films, nucleation and growth of the perovskite phase only occurs from the PZT/Pt interface. At low pyrolysis temperatures, the crystalline nucleation density is much higher in seeded than in unseeded films. The perovskite phase formation process is consequently accelerated by the presence of seeds. PZT thin films with 1 mol % seeds pyrolyzed at 430 °C for 40 h exhibit a dielectric permittivity of 500 and $P_r$ and $E_c$ of 6.71 $\mu$C/cm$^2$ and 80 kV/cm, respectively. Seeded PZT films heat-treated at low temperatures (around 400 °C) may be suitable for applications in which deposition is required onto glass, metallic, or polymeric substrates.

## I. Introduction

$Pb(Zr_xTi_{1-x})O_3$ (PZT) ceramic thin films are of great interest for applications such as transducers and actuators that take advantage of their excellent piezoelectric properties. In addition, ferroelectric random access memories (FERAMs) make use of their reversible polarization under an applied electric field. Techniques for the fabrication of PZT thin films can be divided into two main types: those in which formation of perovskite occurs during deposition and those for which crystallization takes place after deposition. For the former, physical deposition at elevated temperatures (sputtering) and metallorganic chemical vapor deposition (MOCVD) are the main techniques.[1] For the latter, chemical solution deposition (CSD) including sol−gel and MOD (metal−organic decomposition) preparation are the most frequently reported since initial work by Turova and Yanovskaya in the early 1970s.[2] The crystallization temperature of postdeposition heat treatment is a key parameter in the preparation of PZT films. It ensures phase purity and controls interdiffusion between the film and underlayers, which have a direct impact on the final properties of the films. According to earlier reports,[3−11] the typical crystallization temperature for morphotropic PZT films deposited on platinized silicon substrate is as high as 600−700 °C. It is generally accepted that the crystallization temperature of PZT solid solution increases with Zr:Ti ratio. However, the development of a single perovskite phase in PZT films at low temperature is an important issue for property optimization and device performance. At low temperatures, interdiffusion between different layers, undesired chemical reactions, and thermal degradation of the underlying circuit are minimized. Therefore, the reliability of the devices will increase. A low annealing temperature is also required when metallic (not Pt), glass, or polymeric substrates are used.

Various efforts have been undertaken to lower the perovskite crystallization temperature in sol−gel PZT films. By using a lead titanate (PT) seeding layer, the authors of ref 12 decreased the perovskite crystallization temperature to 550 °C for 15 min.[12] With a PT seeded layer plus 50 mol % excess PbO, a single perovskite phase of PZT(53/47) films was obtained on Pt/Ti/SiO2/Si at 500 °C for 2 h.[13] Meanwhile, Huang et al.[14]

* To whom correspondence should be addressed. E-mail: paulas@cv.ua.pt. Tel: (+351) 234 370354. Fax: (+351) 234 425300.
[†] University of Aveiro.
[‡] University of Sheffield.

(1) Fox, G. R.; Krupanidhi, S. B. *J. Mater. Res.* **1994**, *9* (3), 699.
(2) Turova N.; Yanovskaya, M. *Ferroelectric Thin Films*; Paz de Araujo, C., Scott, J. F., Taylor, G. W., Eds.; Gordon & Breach: New York, 1996; p 233.
(3) Budd, K. D.; Dey, S. K.; Payne D. A. *Br. Ceram. Soc. Proc.* **1985**, *36*, 107.
(4) Dey, S. K.; Zuleeg, R. *Ferroelectrics* **1990**, *112*, 309.
(5) Spierings, G. A. C. M.; Ulenaers, M. J. E.; Kampschoer, G. L. M.; van Hal, H. A. M.; Larsen, P. K. *J. Appl. Phys.* **1991**, *70* (4), 2290.
(6) Carim, A. H.; Tuttle, B. A.; Doughty, D. H.; Martinez, S. L. *J. Am. Ceram. Soc.* **1991**, *74* (6), 1455.
(7) Schwartz, R. W.; Assink, R. A.; Headley, T. J. *Mater. Res. Soc. Symp. Proc.* **1992**, *243*, 245.
(8) Tuttle, B. A.; Voigt, J. A.; Goodnow, D. C.; Lamppa, D. L.; Headley, T. J.; Eatough, M. O.; Zender, G.; Nasby, R. D.; Rodgers, S. M. *J. Am. Ceram. Soc.* **1993**, *76* (6), 1537.
(9) Mackenzie, J. D. *J. Sol−Gel Sci. Technol.* **1993**, *1*, 7.
(10) Reaney, I. M.; Brooks, K.; Klissuraka, R.; Pawlaczyk, C.; Setter, N. *J. Am. Ceram. Soc.* **1994**, *77* (5), 1209.
(11) Udayakumar, K. B.; Schuele, P. J.; Chen, J.; Krupanidhi, S. B.; Cross, L. E. *J. Appl. Phys.* **1995**, *77* (8), 3981.
(12) Kwok, C. K.; Desu, S. B. *J. Mater. Res.* **1993**, *8* (2), 339.
(13) Suzuki, H.; Koizumi, T.; Kondo, Y.; Kaneko, S. *J. Eur. Ceram. Soc.* **1999**, *19*, 1397.
(14) Huang, Z.; Zhang, Q.; Whatmore, R. W. *J. Mater. Sci. Lett.* **1998**, *17*, 1157.

10.1021/cm020757k CCC: $25.00 
Published on Web 02/13/2003

reported a crystallization temperature of 440 °C for 100 min for PZT(30/70) films and attributed it to the formation of a $Pt_xPb$ interlayer. More recently, Mandeljc et al.[15] reported crystallization at 400 °C for 5 min, for PZT(30/70) and PLZT(5/30/70), by using 10% excess PbO and either a 10-nm PT or $TiO_2$ nucleation layer. The present authors reported pure perovskite phase formation in PZT(52/48) films at 410 °C for 30 h[16] and 550 °C for 30 min by using seeded diphasic sol−gel precursors.[17]

The kinetics of perovskite crystallization in sol−gel PZT thin films have been studied by several groups.[18−22] Traditionally, these studies have been performed at moderate to high annealing temperatures. Voigt et al.[18] studied the crystallization by rapid thermal annealing (RTA) of PZT(20/80) sol−gel thin films and reported an activation energy of 326 kJ/mol for the perovskite phase formation. Activation energies of 310 and 275 kJ/mol were obtained by Babushkin et al.[19] and Griswold et al.,[20] respectively, for sol−gel-derived PZT(53/47) films. The variation in the activation energy values may arise from different experimental conditions. It has also been reported that the formation of an intermetallic $Pt_xPb$ phase in the early stages of pyrolysis of PZT thin film deposited on $Pt/Ti/SiO_2/Si$ reduces the nucleation activation energy and lowers the temperature for (111)-oriented perovskite PZT formation.[21] Using this effect, an activation energy of 179 kJ/mol was reported for the perovskite phase formation in PZT(30/70) films.[21] The crystallization kinetics of PZT(52/48) seeded and unseeded films was studied by the present authors.[22] The overall activation energy was reduced from 219 kJ/mol (unseeded) to 174 kJ/mol for 1 wt % seeded PZT film and to 146 kJ/mol for 5 wt % seeded films.[22]

A typical columnar-grained microstructure is generally reported for PZT thin films deposited on platinised substrates, as a result of the heterogeneous nucleation of the perovskite phase at the interface of the film/bottom electrode and grain growth through the film that consumes the matrix.[10,23−29] In columnar-grained films, the (111) PZT orientation is maximized. The preferred (111) orientation has been attributed to the (111) orientation of the Pt electrode, aided by the formation of either $Pt_xPb$[30] or $Pt_3Ti$[31] transient phases. These phases have lattice parameters closer to that of PZT and so they may also act as nucleation sites ($d_{111}Pt_3Ti$ = 0.2244 nm, $d_{111}Pt_xPb$ = 0.2340 nm, $d_{111}PZT(52/48)$ = 0.2351 nm). Their formation, during the processing of PZT films, is not always observed and depends on the experimental conditions applied.

It is evident from the literature that there have been few studies of the phase evolution of PZT films at temperatures normally considered suitable for pyrolysis (350−450 °C) rather than crystallization (600 °C). At high annealing temperatures (600−700 °C for RTA) all reactions including organic decomposition, combustion, and crystallization have already occurred and any intermetallic layers[30−32] have disappeared. Consequently, their conditions of formation and relationship with the development of film texture are not well-understood. However, at low temperature (∼400 °C), all the above reactions are slower and may be studied systematically as a function of time. Understanding the mechanisms involved in the nucleation and growth of perovskite PZT is of vital importance in optimizing sol−gel processing conditions and reducing processing temperature.

In the present work, the crystallization, structure, and microstructural development and electrical properties have been investigated in PZT films heat-treated at low temperatures (∼400 °C). The films are prepared on Pt-passivated silicon substrates by a modified sol−gel route, developed by the authors, in which different concentrations of nanometric PZT powders are dispersed in the sol. From previous work, besides the reduction of the overall activation energy for the perovskite phase formation in seeded films,[22] an improved microstructure was obtained.[17] Seeded PZT films on platinized substrates show a lesser degree of orientation along the (111) direction and an improvement in ferroelectric and fatigue properties.[33] In these studies, the formation of the metastable intermetallic $Pt_xPb$ interlayer, between the film and the Pt electrode layer, was also observed. The formation of $Pt_xPb$ is minimized or even suppressed in seeded films and the thickness and stoichiometry of the $Pt_xPb$ layer varied with the concentration of seeds and heat treatment of the film.[23] Nonetheless, direct evidence of the role of seeds on perovskite phase nucleation and growth has not been observed yet. Therefore, a systematic study of crystallization has been performed to understand how seeds affect the mechanism of perovskite nucleation and growth in PZT thin films. XRD and TEM have been used to compare films in the early stages of pyrolysis to establish a correlation between film morphology and texture. The corresponding electrical properties of films heat-treated at ∼400 °C are presented.

(15) Mandeljc, M.; Kosec, M.; Malic, B.; Samardzija, Z. *Integr. Ferroelectr.* **2000**, *30*, 149.
(16) Wu, A.; Miranda Salvado, I. M.; Vilarinho, P. M.; Baptista, J. L. *J. Eur. Ceram. Soc.* **1997**, *17*, 1443.
(17) Wu, A.; Vilarinho, P. M.; Miranda Salvado, I. M.; Baptista, J. L.; De Jesus, C. M.; Da Silva, M. F. *J. Eur. Ceram. Soc.* **1999**, *19*, 1403.
(18) Voigt, J. A.; Tuttle, B. A.; Headley, T. J.; Eatough, M. O.; Lamppa, D. L.; Goodnow, D. *Mater. Res. Soc. Symp. Proc.* **1993**, *310*, 15.
(19) Babushkin, O.; Lindbäck, T.; Brooks, K.; Setter, N. *J. Eur. Ceram. Soc.* **1997**, *17*, 813.
(20) Griswold, E. M.; Weaver L.; Calder, I. D.; Sayer, M. *Mater. Res. Soc. Symp. Proc.* **1995**, *361*, 389.
(21) Huang, Z.; Zhang, Q.; Whatmore, R. W. *J. Appl. Phys.* **1999**, *85* (10), 7355.
(22) Wu, A.; Vilarinho, P. M.; Reaney, I. M.; Miranda Salvado, I. M.; Baptista, J. L. *Integr. Ferroelectr.* **2000**, *30*, 261.
(23) Wu, A.; Vilarinho, P. M.; Miranda Salvado, I. M.; Baptista, J. L.; Zhou Z.; Reaney, I. M.; Ramos, A. R.; Da Silva, M. F. *J. Am. Ceram. Soc.* **2002**, *85* (3), 641.
(24) Huffman, M.; Zhu, J.; Al-Jassim, M. M. *Ferroelectrics* **1993**, *140*, 191.
(25) Carim A. H.; Tuttle, B. A.; Doughty, D. H.; Martinez, S. L. *J. Am. Ceram. Soc.* **1991**, *74* (6), 1455.
(26) Myers, S. A.; Chapin, L. N. *Mater. Res. Soc. Symp. Proc.* **1990**, *200*, 231.
(27) Lakeman, C. D. E.; Xu, Z.; Payne, D. A. *J. Mater. Res.* **1995**, *10* (8), 2042.
(28) Zhu, W.; Liu, Z. Q.; Lu, W.; Tse, M. S.; Tan, H. S.; Yao, X. *J. Appl. Phys.* **1996**, *79* (8), 4283.
(29) Kaewchinda, D.; Chairaungsri, T.; Naksata, M.; Milne, S. J.; Brydson, R. *J. Eur. Ceram. Soc.* **2000**, *20*, 1277.
(30) Chen, S. Y.; Chen, I-W. *J. Am. Ceram. Soc.* **1994**, *77* (9), 2332.
(31) Tani, T.; Xu, Z.; Payne, D. A. *Ferroelectr. Thin Films III, Mater. Res. Soc. Symp. Proc.* **1993**, *310*, 269.
(32) Gardeniers, J. G. E.; Elwenspoek, M.; Cobianu, C. *Mater. Res. Soc. Symp. Proc.* **1994**, *343*, 451.
(33) Wu, A.; Vilarinho, P. M.; Kholkin, A. L.; Miranda Salvado, I. M.; Baptista, J. L. *Integr. Ferroelectr.* **2001**, *37* (1−4), 475.

## II. Experimental Section

PZT(52/48) seed powder was prepared by a sol−gel process, as described elsewhere.[34] To avoid the formation of hard aggregates during calcination, the PbOAc−ZrAcAc−TIAA route[34] was used, in which lead acetic acid (99.5%, Riedel-de Haën), zirconium acetyl acetonate (98%, Merck), and titanium diisopropoxide acetyl acetonate (75%, Aldrich) were chosen as source reagents. The seeds were precalcined at 600 °C for 1 h and the presence of perovskite phase was confirmed by using XRD and TEM. The PZT powder was dispersed in 1,2-propanediol and acetone solution, by vibration milling in a Teflon pot using yttrium-stabilized zirconia balls. To obtain a stable PZT seed suspension, surfactants, such as Dispex A40 (ammonium salt of polycarboxylic acid, Allied Colloids Ltd.) and/or Hypermer KD2 (polymeric surfactant, ICI Colour & Fine Chemicals), were added. A 0.4 M PZT precursor sol was also prepared by sol−gel. The ratio of Pb:Zr:Ti was kept at 1:0.52:0.48. Lead acetate trihydrate was dissolved in 1,2-propanediol and acetic acid.

Zirconium tetra-*n*-propoxide stabilized with acetic acid and 1,2-propanediol was added to the lead solution followed by titanium tetra-isopropoxide stabilized with acetylacetone. Acetone was finally used to dilute the PZT precursor sol to a 0.4 M stock sol. Seeded diphasic PZT sols were prepared by mixing PZT seeds and the PZT precursor sol so that the concentration of seeds in the seeded precursor sol was 1 and 5 mol % of PZT in the sol. A high-intensity ultrasonic liquid processor (Vibra cell, Model VC-50, Sonics & Materials Inc.) was used to help disperse the seeds.

The substrates used for this investigation were Pt-covered Si monocrystal ($Pt/Ti/SiO_2/Si$). Just before the deposition, the suspension was sonicated for 20 min. PZT(52/48) films were prepared by dip coating using a withdrawal speed of 1.7 mm/s. The gel films were dried at 300 °C for 1 min to remove the organics. This procedure was repeated four times to achieve a final film thickness of about 300 nm, determined by scanning electron microscopy (SEM, Hitachi S-4100). The as-dried films were directly inserted into a hot furnace at the set temperature. The films were fired in a tube furnace at a temperature of 400 °C for 5 min to 40 h, in air.

Transmission electron microscopy (TEM, Hitachi H9000-NA) and scanning electron microscopy, both coupled with energy-dispersive spectroscopy (EDS) and XRD (Rigaku, D/Max-B) analyses, were used to characterize the structure and microstructure of the films. Cross sections were prepared for ion-milling following the technique described by Reaney et al.[10] Thinning to electron transparency was performed using an $Ar^+$ ion-miller (BAL-TEC, RES-100) operated at 5−6 kV at an incidence angle of 8−9°.

Capacitance and loss factor of the films versus frequency were measured using a Solartron 1260 impedance/gain-phase analyzer. Dielectric hysteresis loops were acquired using a TFA analyzer (AIXACCT, Model: TFA-LI).

## III. Results and Discussion

**(a) As-Dried Films.** Figure 1 shows the XRD patterns for as-dried seeded and unseeded films. All samples are largely amorphous according to XRD but a broad peak corresponding to the perovskite phase was observed for the 5 mol % seeded film.[22] This was attributed to the crystalline perovskite seeds dispersed in the film. SEM micrographs of lead zirconate titanate films before pyrolysis show flat homogeneous films with no characteristic features for either unseeded or seeded films. Therefore, to further investigate as-dried films, TEM was performed on cross sections of samples. Figure 2a corresponds to the unseeded film before pyrolysis and the inset is the electron diffraction (ED) pattern taken in the PZT film area. An amorphous microstructure can be observed as illustrated by the morphology of the image and the halo ED pattern (inset Figure 2a). The small black dots superimposed over the homogeneous background are probably due to the formation of amorphous Pb and/or PbO particles homogeneously distributed throughout a $Ti(Zr)O_2$ matrix that have formed during irradiation in the electron beam. Small Pb-rich particles, 4−8-nm diameter, were also observed by other authors in as-prepared CVD lead titanate thin films.[35] Figure 2b shows the microstructure of a cross section of the as-dried 5 mol % seeded films, in contrast with unseeded films, some nanometric particles which gave rise to discrete reflections in ED patterns (inset of Figure 2b). The main *d* spacing calculated from individual diffraction spots are 4.105, 2.89, 2.79, 2.36, 2.05, 1.81, 1.66, and 1.47, which corresponds to the (100), (101), (110), (111), (002), (201,210), (211), and (022) reflections of the perovskite structure. It was concluded, therefore, that the nanometric particles were perovskite seed crystals distributed throughout the bulk of the film, confirming the XRD data (Figure 1).

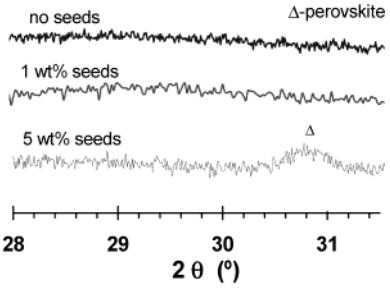


**Figure 1.** XRD patterns of as-dried PZT films.

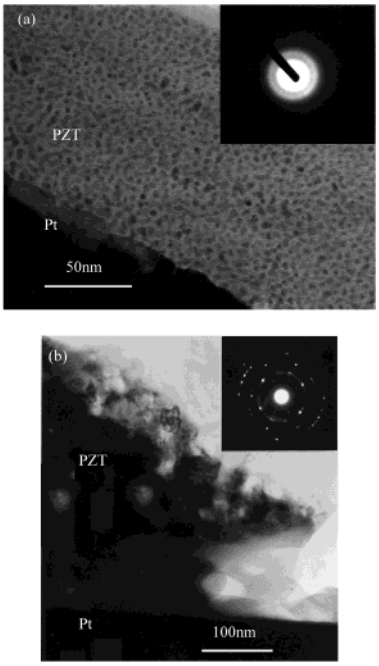


**Figure 2.** TEM cross section of as-deposited (before pyrolysis) PZT film without (a) and with 5 mol % of seeds (b).

**(b) Heat-Treated Films.** Figure 3 shows the XRD patterns from unseeded and seeded films heat-treated

(34) Wu, A.; Miranda Salvado, I. M.; Vilarinho, P. M.; Baptista, J. L. *J. Am. Ceram. Soc.* **1998**, *81* (10), 2640.

(35) Leinen, D.; Caballero, A.; Fernández, A.; Espinós, J. P.; Justo, A.; González-Elipe, A. R.; Martin, J. M.; Maurin-Perrier, B. *Thin Solid Films* **1996**, *272*, 99.

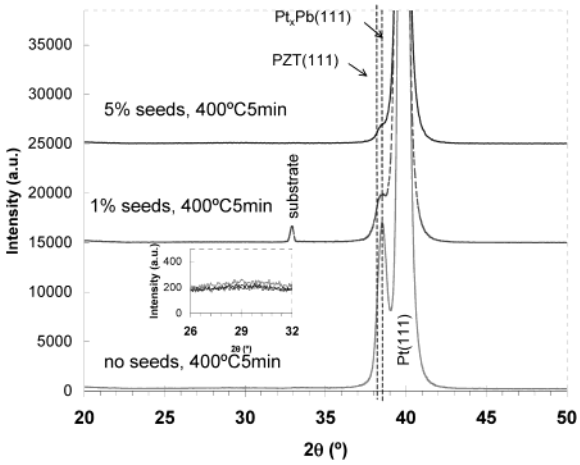


**Figure 3.** XRD patterns of PZT films pyrolyzed at 400 °C/5 min.

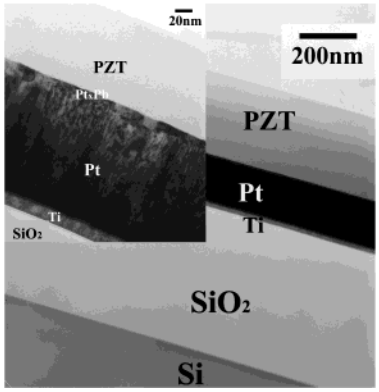


**Figure 4.** TEM cross section of unseeded PZT film after pyrolysis at 400 °C/5 min.

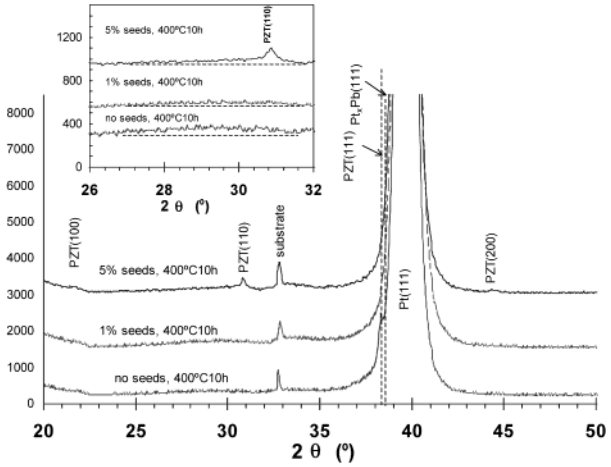


**Figure 5.** XRD patterns of PZT films pyrolyzed at 400 °C/10 h.

at 400 °C/5 min. After 5 min, the PZT phase in both unseeded and seeded films is still amorphous, exhibiting a broad hump at 30.9° (2$\theta$). However, a well-defined peak at 38.5° (2$\theta$) corresponding to a Pb$_x$Pt(111) phase is present in patterns from unseeded films. This peak diminishes in relative intensity but remained for up to 5 h at 400 °C; at which time it disappeared to be replaced by a peak at a slightly lower 38.2° (2$\theta$) value, attributed to perovskite(111). Although seeded films also exhibited a peak associated with Pb$_x$Pt(111) after 5 min at 400 °C, its intensity decreased as a function of

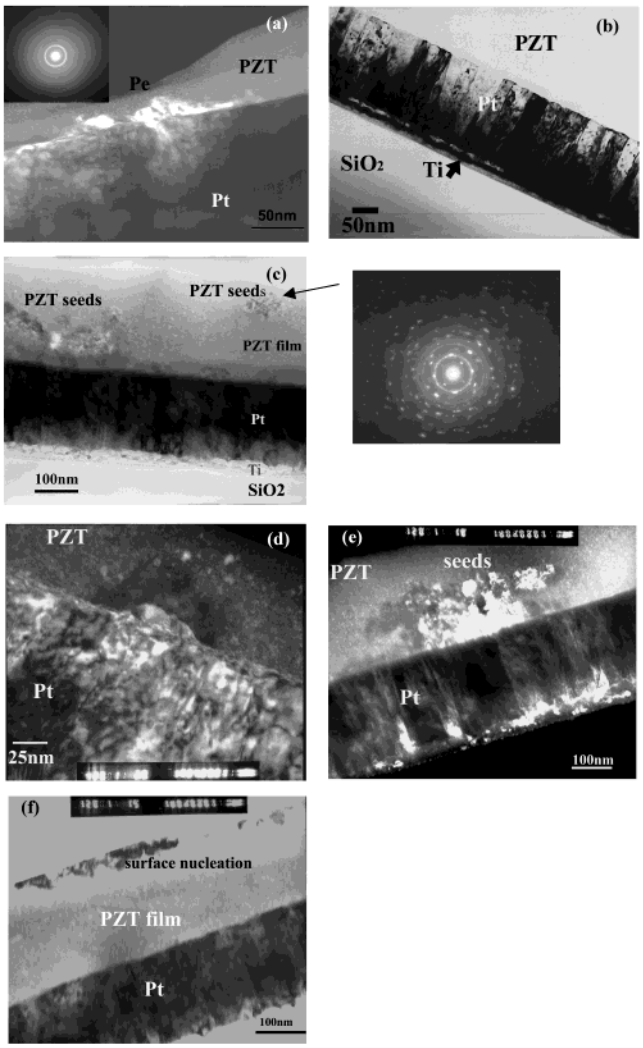


**Figure 6.** TEM analysis of unseeded film (a, b) and seeded PZT films (c−f) after pyrolysis at 400 °C/10 h.

increasing seed concentration until almost absent for 5 mol % seeded film (Figure 3).

Figure 4 shows a TEM cross section of an unseeded film, pyrolyzed at 400 °C for 5 min. In agreement with XRD data, the film appears amorphous and exhibits ED patterns similar to the inset in Figure 2a. However, at the Pt/PZT interface, inset of Figure 4, a Pt$_x$Pb interlayer is clearly observed, consistent with other reports.[14,29,30] For seeded films pyrolyzed under the same conditions, a Pt$_x$Pb interlayer is not observed, although the XRD pattern shows trace amounts of this phase.

Figure 5 shows the XRD patterns from unseeded and seeded films heat-treated at 400 °C for 10 h. Peaks associated with the Pb$_x$Pt layer are no longer present. For unseeded films, a small peak corresponding to the perovskite PZT(111) is observed, together with a broad bump around 29° (2$\theta$), attributed to the pyrochlore phase. For 5 mol % seeded films, several peaks corresponding to the perovskite phase (100), (110), and (200) reflections are clearly seen and no obvious pyrochlore phase was detected.

TEM cross sections of unseeded and seeded films after pyrolysis at 400 °C for 10 h are shown in Figure 6. Figure 6a is a dark field image of part of an unseeded film. Perovskite PZT has nucleated from the bottom electrode/PZT interface. The observation of the interface

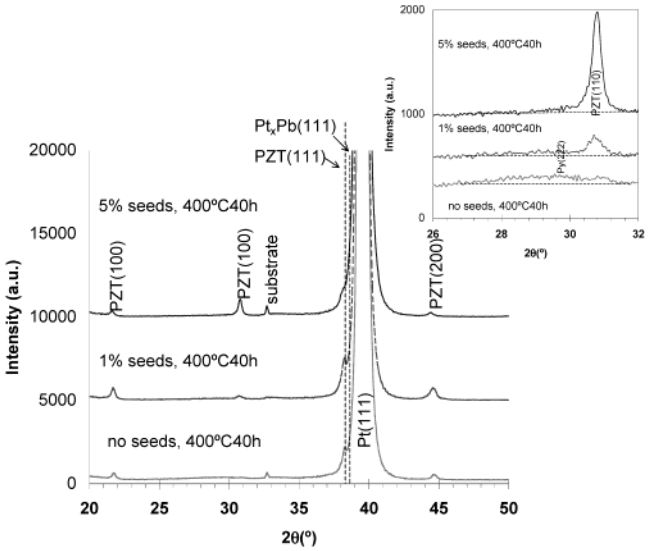


**Figure 7.** XRD patterns of PZT films pyrolyzed at 400 °C/40 h.

layers of the substrate revealed that, even at temperatures as low as 400 °C, Ti can interdiffuse into a Pt layer, as shown in Figure 6b. But the interdiffusion is limited to the Ti/Pt interface and does not penetrate through the Pt layer to form $Pt_3Ti$ on the Pt surface. No titanium was detected on the interface of Pt/PZT, by EDS analysis. The nucleation of the $Pt_3Ti$ interlayer, as reported by some authors,[31,36] is excluded in current experimental conditions.

Parts c−f of Figure 6 are TEM images obtained from cross sections of 5 mol % seeded films after pyrolysis at 400 °C for 10 h. Compared to unseeded films heat-treated under the same conditions, the extent of crystallization to the perovskite phase is clearly greater, as evidenced by the greater volume fraction of material crystalized to the perovskite phase (see ED pattern inset in Figure 6c). PZT perovskite crystallites are identified in several places of the film: dispersed in the bulk of the film (Figure 6c), near the bottom interface film/electrode (Figure 6d,e) and near the surface (Figure 6f). Contrary to unseeded films and according to these TEM images, the nucleation and growth of PZT crystals in seeded films occurs simultaneously at the surface of the seeds dispersed in the bulk of the film, at the bottom electrode interface, and at the surface of the film. The occurrence of perovskite surface nucleation in sol−gel-derived PZT films at high temperatures has been reported by other authors,[37−38] but its occurrence at such a low temperature was not reported, to the the best of the authors' knowledge.

Figure 7 shows the XRD patterns from unseeded and seeded films after pyrolysis at 400 °C for 40 h. In general, as the pyrolysis time increases, the amorphous film transforms into the perovskite phase with residual pyrochlore phase detected in unseeded films at 29° (2$\theta$) Moreover, unseeded films show a pronounced PZT(111) peak, a weak PZT(100) peak, and a small hump at 30.9° (2$\theta$) of PZT(110) peak, indicating a strong (111) preferred orientation. For 1 mol % seeded films, PZT(111), (100), and (110) peaks have a greater relative intensity than those in unseeded films. The higher total intensity of the peak area of (100), (110), and (111) peaks indicates a higher degree of crystallinity (to the

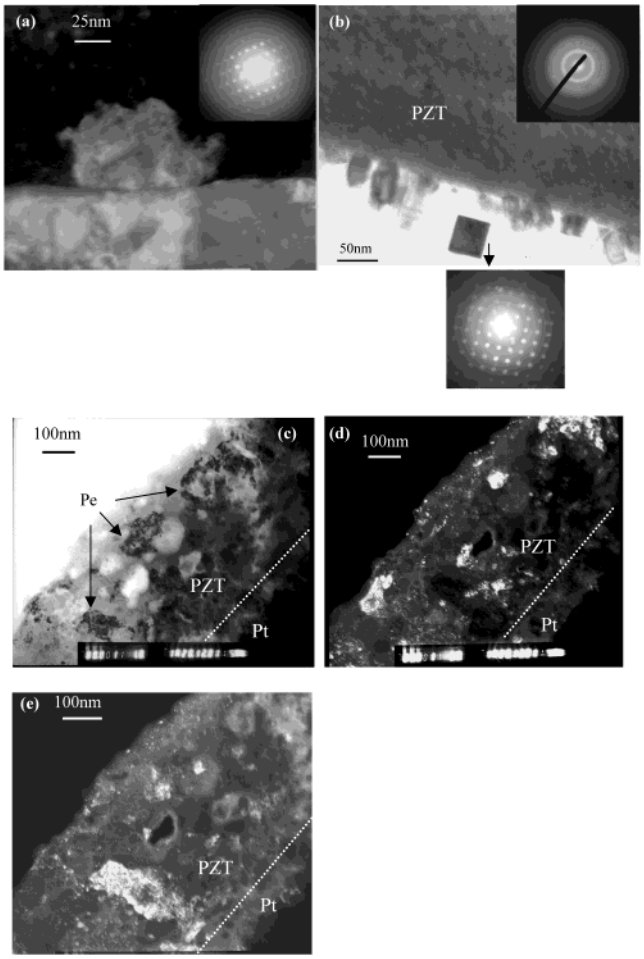


**Figure 8.** TEM analysis of unseeded film (a, b) and seeded PZT films (c−e) after pyrolysis at 400 °C/40 h.

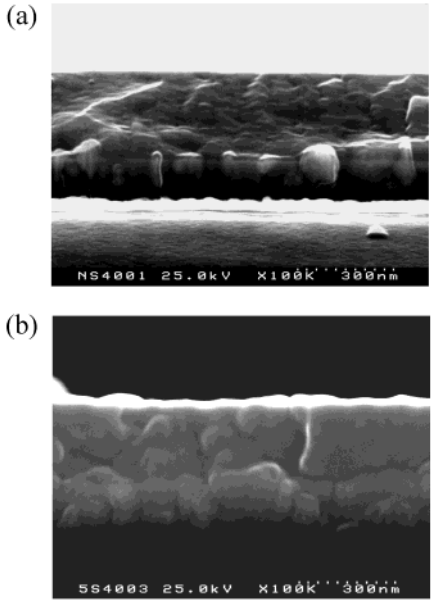


**Figure 9.** SEM cross section of unseeded film (a) and seeded PZT film (b) after pyrolysis at 400 °C/40 h.

(36) Muralt, P.; Maeder, T.; Sagalowicz, L.; Hiboux, S.; Xanthopoulos, N.; Mathieu, H. J.; Patthey, L.; Bullock, E. L. *J. Appl. Phys.* **1998**, *83* (7), 3835.
(37) Brooks, K. G.; Reaney, I. M.; Klissurska, R.; Huang, Y.; Bursill, L.; Setter, N. *J. Mater. Res.* **1994**, *9* (10), 2540.
(38) Seifert, A.; Sagalowicz, L.; Muralt, P.; Setter, N. *J. Mater. Res.* **1999**, *14* (5), 2012.

**Table 1. Summary of Early Stage Crystallization Studies of PZT Thin Films on Pt-Covered Silicon Substrates[a]**

| heat treatment | phases | seeded film | unseeded film |
|---|---|---|---|
| without heat treatment (as-deposited) | $Pt_xPb$ | not observed by TEM<br>not observed by XRD | not observed by TEM<br>not observed by XRD |
| | $P_e$ | observed by TEM (seed particles)<br>observed by XRD (seed particles) | not observed by TEM<br>not observed by XRD |
| | $P_y$ | not observed by TEM<br>not observed by XRD | not observed by TEM<br>not observed by XRD |
| 400 °C/5 min | $Pt_xPb$ | not observed by TEM<br>observed by XRD | observed by TEM<br>observed by XRD |
| | $P_e$ | observed by TEM (seed particles)<br>observed by XRD (seed particles) | not observed by TEM<br>not observed by XRD |
| | $P_y$ | not observed by TEM<br>not observed by XRD | not observed by TEM<br>not observed by XRD |
| 400 °C/15 min | $Pt_xPb$ | not observed by TEM<br>observed by XRD<br>(only in 1 mol % seeded film) | observed by TEM<br>(much thinner layer)<br>observed by XRD |
| | $P_e$ | observed by TEM (seed particles)<br>observed by XRD | not observed by TEM<br>not observed by XRD |
| | $P_y$ | not observed by TEM<br>observed by XRD | not observed by TEM<br>observed by XRD |
| 400 °C/10 h | $Pt_xPb$ | not observed by TEM<br>not observed by XRD | not observed by TEM<br>not observed by XRD |
| | $P_e$ | observed by TEM (Pe nuclei on film surface, bulk film, and bottom Pt layer)<br>observed by XRD | observed by TEM<br>(only bottom nucleation)<br>observed by XRD |
| | $P_y$ | not observed by TEM<br>observed by XRD<br>(very weak reflection) | observed by TEM<br>observed by XRD |
| 400 °C/40 h | $Pt_xPb$ | not observed by TEM<br>not observed by XRD | not observed by TEM<br>not observed by XRD |
| | $P_e$ | observed by TEM<br>(Pe nuclei on film surface, bulk film, and bottom Pt layer)<br>observed by XRD<br>grain growth from both bottom nucleation and inside the bulk of the PZT film, columnar grain interrupted by some randomly distributed grains, specially in 5 mol % seeded films | observed by TEM<br>(only bottom nucleation)<br>observed by XRD<br>grain growth only from nuclei near the bottom interlayer, columnar growth effect |
| | $P_y$ | not observed by TEM<br>not observed by XRD | observed by TEM (not clear)<br>cubic-shaped surface crystals of PbO observed by TEM; EDS-confirmed lead nature<br>observed by XRD<br>(weak humble reflection) |

[a] $Pt_xPb$: metastable interlayer appeared during the crystallization process of PZT film on a Pt-covered substrate, confirmed by XRD and TEM EDS analysis. $P_e$: perovskite phase. $P_y$: pyrochlore phase.

perovskite phase). As the seed content increases to 5 mol %, the PZT(111) preferred orientation is lost and a pronounced (110) peak is observed; 5 mol % seeded film exhibits the highest degree of crystallinity. The inset of Figure 7 illustrates that little pyrochlore phase is residual in unseeded film but absent in 5 mol % seeded films.

Figure 8 shows a series of TEM images of cross sections of microstructures of pyrolyzed unseeded and seeded films heat-treated for 40 h at 400 °C. Figure 8a is a TEM dark field image of an unseeded film pyrolyzed at 400 °C for 40 h. Perovskite crystal growth has occurred from the film/Pt electrode interface, giving a columnar grain structure, consistent with results reported for PZT films treated at high temperatures for shorter times. Meanwhile, lead-rich cubic crystals have been observed on the top surface of the PZT film (400 °C/40 h) (Figure 8b), which may be caused by condensation of lead vapor, due to long pyrolysis time, or by an artifact of ion-milling. SEM images of the film (Figure 9) do not show any clear grains on the surface but they may be indistinguishable from the general PZT microstructure. Parts c and d of Figure 8 are TEM images of 5 mol % seeded films pyrolyzed at 400 °C for 40 h. The columnar microstructure observed in Figure 8a (unseeded) is no longer apparent (Figure 8c), and there is evidence that nucleation has occurred from the films surface, PZT/Pt electrode interface and in the bulk on seeds (Figure 8d,e). These observations are consistent with images obtained from seeded samples heat-treated for 10 h at 400 °C and also with the decrease in relative intensity of the PZT(111) peak in seeded films compared with unseeded films.

Table 1 summarizes the TEM and XRD results of the current study. These results are the experimental evidence that the presence of randomly oriented PZT seeds dispersed in the film supplies additional crystalline nucleation and growth sites. Consequently, the

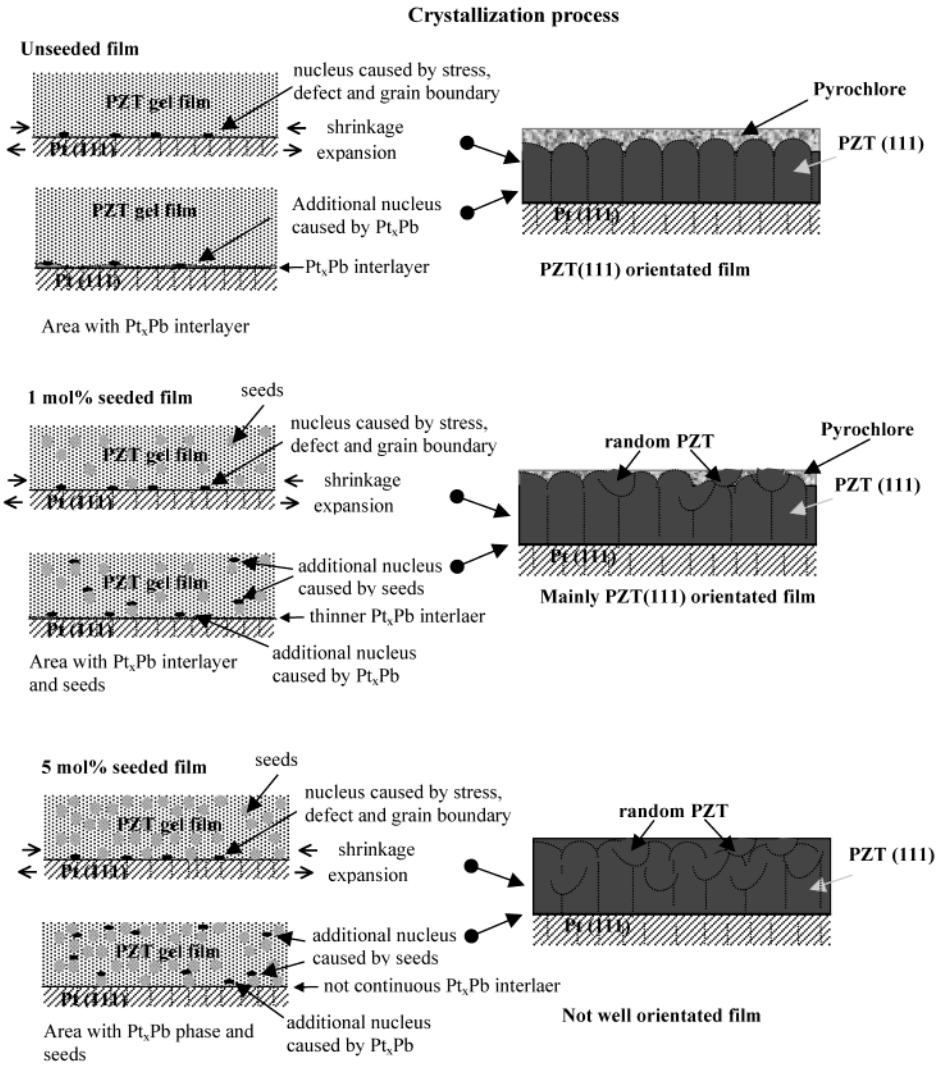


**Figure 10.** Schematic illustration of perovskite nucleation and growth process in unseeded and seeded PZT films.

perovskite phase crystallization is enhanced and the pyrochlore phase is suppressed. At the same time the formation of the $Pb_xPt$ interlayer is also suppressed and further decreasing of the (111) preferred growth of the perovskite phase. The literature reports that the reduction of this interlayer will increase the activation energy of perovskite phase formation.[21] In the present study this was supplemented by the presence of seeds, which act as additional perovskite growth sites to facilitate perovskite phase formation.

The above difference between seeded and unseeded films microstructure suggests that a different crystal nucleation and growth process takes place in these films. The formation of thermal stresses between the film and the substrate during the heat treatment, and the interlayers of $Pt_xPb$, $Pt_3Ti$ and Pt(111), have been thought to be the driving force for perovskite PZT(111) nucleation and growth.[10,14,30,36,39] In current work, the formation of $Pt_3Ti$ is excluded, but the effects of $Pt_xPb$ interlayer and thermal stresses, caused by the expansion of Pt and shrinkage of PZT gel film, cannot be neglected since all the films retain to some extent the (111) preferred orientation. Furthermore, the extent of orientation decreases with decreasing interlayer intensity in seeded films. Also, defects and/or grain boundaries of the platinum layer also act as nucleation sites. In the current situation, it is assumed that this effect is the same in seeded and unseeded films since the substrate and the pyrolysis conditions are the same. Considering these effects and the presence of seeds, the postulated nucleation and growth mechanisms for seeded and unseeded films is schematically depicted in Figure 10. Heterogeneous nucleation occurs on different interfaces in seeded films, that is, at the surface of the bottom electrode, at the seed surfaces, and at the top film surface. This results in a higher degree of perovskite crystallinity for a given set of processing conditions but a less orientated texture. Comparatively, in unseeded films the nucleation takes place only at the surface of the bottom electrode; a preferred orientation is obtained. These microstructural observations are consistent with kinetic studies performed on similar samples in which seeded films had a lower activation energy.

Compositional homogeneity through the film thickness can be strongly influenced by the crystalline growth mechanism. Reaney et al.[10] reported that for sol−gel PZT films, in which the perovskite phase nucleates from the bottom electrode, Zr preferentially diffuses toward the film surface as crystallization proceeds. In turn, the crystalline growth rate decreases because the activation

(39) Liu, Y.; Phulé, P. P. *J. Am. Ceram. Soc.* **1996**, *79* (2), 495.

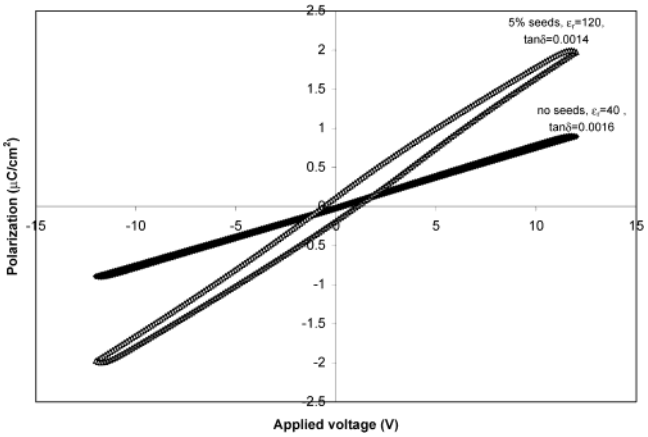


**Figure 11.** Hysteresis loops and dielectric constant of PZT films heat-treated at 400 °C/30 h measured at room temperature.

energy of Zr-rich PZT is greater than that of $PbTiO_3$, and the increased Zr concentration at the growth front increases the stability of the metastable pyrochlore phase. This can lead to the occurrence of a residual pyrochlore phase on the film surface and strongly degrades the film electric properties.[37] In seeded films, the perovskite nucleation occurs also in the bulk and at the film−air interface, before zirconium partitioning and Pb diffusion can occur, thereby keeping greater compositional homogeneity and facilitating perovskite crystallization.

PZT films prepared with seeds in this study are compact and homogeneous, and in principle the crystallization mechanisms discussed above should give rise to films with electrical properties superior to unseeded films. Figure 11 shows the dielectric constant, dielectric loss, and hysteresis loops of unseeded and 5 mol % seeded films pyrolyzed at 400 °C for 30 h, measured at room temperature. An incipient hysteresis loop was observed in 5 mol % seeded film with a dielectric constant of 120 (Figure 11). Unseeded films exhibit a relatively lower dielectric constant of 40 and no hysteresis loop was observed. Figure 12a depicts the dielectric constant and dielectric loss versus frequency of unseeded and seeded films pyrolyzed at 430 °C for 40 h, measured at room temperature. XRD results of these films show a higher degree of crystallinity of perovskite phase in both seeded and unseeded films than those pyrolyzed at 400 °C for 30 h, but unseeded film still show residues of pyrochlore phase. As expected, seeded film shows higher dielectric constant (around 460−500) over the measuring frequency range. Figure 12b displays the hysteresis loops of the same films, measured at 100 Hz at room temperature. The $P_r$ and $E_c$ are 6.71 $\mu$C/cm$^2$ and 80 kV/cm, respectively. Still no hysteresis loop is observed for unseeded films pyrolyzed at these low temperatures. These electric measurements of PZT films are very consistent with their microstructure characteristics.

## IV. Conclusions

The early stages of heat treatment of lead zirconate titanate (PZT) thin films prepared by sol−gel with diphasic precusor sols were studied. Detailed TEM and

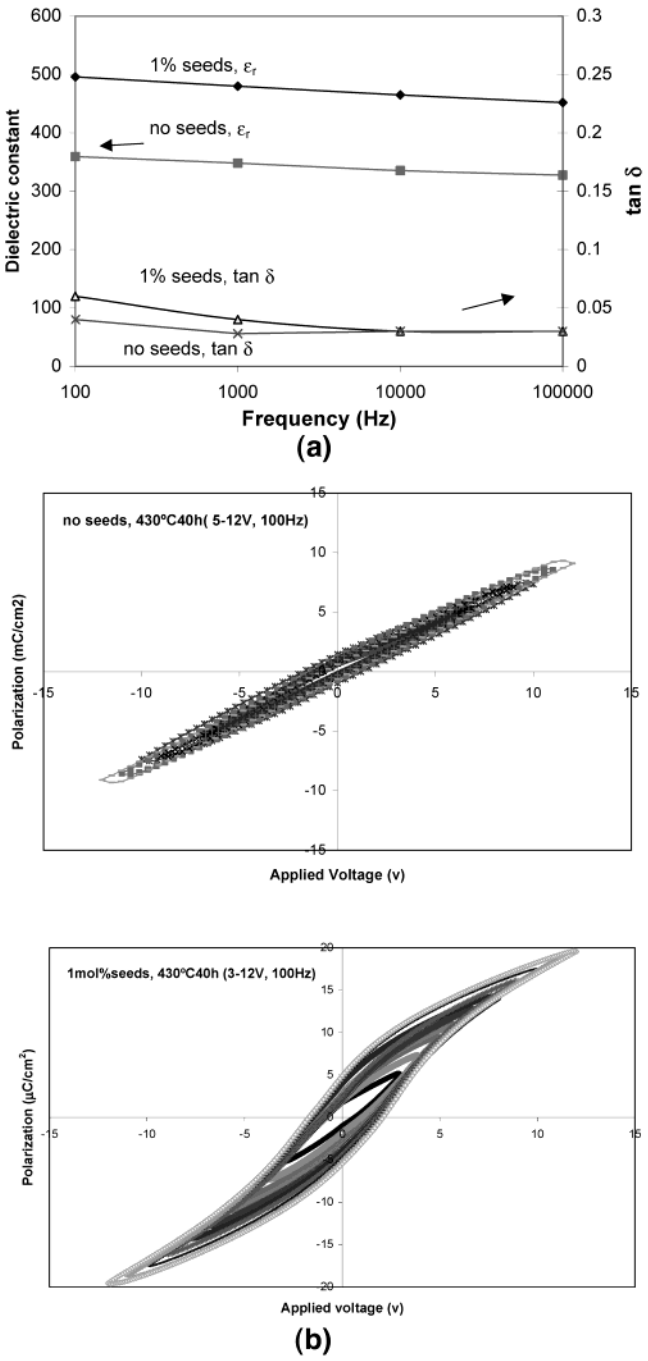


**Figure 12.** (a) Dielectric permittivity versus frequency of PZT films heat-treated at 430 °C/40 h. (b) Hysteresis loops measured at room temperature for unseeded (up graph) and 1 mol % seeded (down graph) PZT films heat-treated at 430 °C/40 h.

XRD analysis results revealed that perovskite phase nucleates and grows from the film−air interface, surface of the seeds, and interface of the film−bottom electrode layer in seeded films. In contrast, perovskite nucleation in unseeded films only occurs from the bottom Pt electrode under the same pyrolysis conditions. In addition, the use of seeds encourages a greater nucleation density. The observed local random perovskite nucleation and the decrease of the $Pt_xPb$ phase formation are considered responsible for the decreased (111) PZT crystalline texture in seeded films. The higher degree of crystallinity and homogeneity of the microstructure

of seeded films pyrolyzed at low temperatures is patent in the observed dielectric and ferroelectric properties of these films. Seeded PZT thin films pyrolyzed at 430 °C for 40 h with a dielectric permittivity of 500 and $P_r$ and $E_c$ of 6.71 $\mu$C/cm$^2$ and 80 kV/cm, respectively, are well-suited for applications in which glass, metallic, or polymeric (such as polyimide family type) substrates are required.

**Acknowledgment.** The authors would like to thank Dr. Zhaoxia Zhou, Department of Engineering Materials, University of Sheffield, for the experiment assistance in TEM. A maintenance scholarship from FCT, Portugal (Praxis XXI BPD/20196/99) for A. Wu is acknowledged.

CM020757K